Hindawi
Mobile Information Systems
Volume 2022, Article ID 2893172, 14 pages
https://doi.org/10.1155/2022/2893172

Research Article

Surface Movement and Deformation Law Caused by Different Coal Pillar Stagger Distances in Strip Filling IoT-Enabled Sustainable Mining

Yuanhao Zhu,[1] **Yanjun Zhang**,[1] **Jiayuan Kong**,[1] **and Qian Yang**[2]

[1]*College of Geoscience and Surveying Engineering, China University of Mining and Technology-Beijing, Beijing 100083, China*
[2]*Xinhuasan Group Co., Ltd, Beijing 100022, China*

Correspondence should be addressed to Yanjun Zhang; bqt2100204049@student.cumtb.edu.cn

Received 23 June 2022; Revised 6 July 2022; Accepted 11 July 2022; Published 10 August 2022

Academic Editor: Muhammad Zakarya

Most of the mines in the middle and lower reaches of the Yellow River Basin in China have the occurrence characteristics of multiple coal seams, and the mining is easy to cause damage to the ecological and human settlement environments. Mine monitoring methods, using Internet of Things (IoT) and machine learning, pursue to develop a suitable atmosphere to avoid similar damages and mine closure with supreme efficacy. Accurate monitoring methods reduce these damages and optimize mining. Strip filling mining is characterized by high efficiency, reliability, and low cost, which provides a good technical support for mining damage control. However, how to reasonably layout the working face under multicoal seam conditions and the law of surface movement under different coal pillar stagger distance need to be studied. Based on the geological and mining conditions of a mine in Shandong Province, through numerical simulation and theoretical analysis, this article studies the influence of coal pillar stagger distance on surface movement of multicoal seam strip filling mining. The study reveals mechanism for surface cooperative deformation under different coal pillar stagger distances. Furthermore, an IoT, cloud computing, and data aggregation based architecture is offered in order to support the development of a digital and sustainable mining platform. The results show that the surface subsidence is positively correlated with coal pillar stagger coefficient and mining layers. When the stagger coefficient $s \geq 0.75$, then the surface subsidence and horizontal movement are less affected by the change of coal pillar stagger coefficient. The relationship between surface subsidence ratio and coal pillar stagger coefficient, in multicoal seam strip filling mining, is a power function. The subsidence ratio observed was 0.21–0.32, and the horizontal movement coefficient is about 0.09. The fitting empirical formula of surface subsidence ratio and coal pillar stagger coefficient, in this particular mining area, is established through various machine learning methods. Under the mining conditions of gently inclined coal seam, the surface subsidence can be slowed down to a certain extent by the arrangement of working face along incline direction. Through plausible assumption, our experimental outcomes demonstrate that the proposed prototype can improve the prediction accuracy and model execution times, from 14.2% to 18.9%, through the data aggregation method.

1. Introduction

The Yellow River Basin is rich in coal resources, which is the most significant base of coal production in China and also an important ecological barrier in China [1]. However, the exploitation of an enormous number of coal resources inevitably consequences to a series of ecological environmental damages and human settlement environmental damages. In particular, the repeated disturbance, long duration, and large destructiveness of multicoal seam mining are some of the common damages, which have a great negative impact on local people and ecological environment [2]. Source subsidence control mining and environmental posttreatment are the keys to ensure green and sustainable development of human settlements and ecological environment in mining areas. In fact, the former one is the most direct and important technical approach. Many researchers have accomplished relevant research work. The essence of source

subsidence control mining is to use "three under" coal mining technology to control strata, including strip mining, filling mining, and so on.

As a partial mining technology [3], strip mining has good subsidence control effect and is widely used. Zou et al. [4] proposed the three-dimensional layered medium theory of strip mining and the main control factors of surface movement control, and established the elastic mechanics model of strip mining. Similarly, Wang et al. [5] extended the work for the limitations of the application of A. H. Wilson design theory, given that the formula is not constrained by geological mining conditions. Guo [6] proposed the probability integral superposition prediction method of full-mining multiface according to the characteristics of deep large mining width strip mining. The proposed prediction methods can more accurately predict the deformation and surface movement of deep strip mining. Yu et al. [7, 8] established the strip coal pillar nonuniform stripping model, and proposed the strip coal pillar long-term stability field evaluation method. Strip mining is also the main technical means of multicoal seam mining. Moreover, Deng et al. [9] studied the connection among the spatial position of multicoal pillar and the movement of overlying strata and surface, and gave the corresponding functional relationship. Similarly, Zhang [10] used the method of similarity and numerical simulations in order to reveal the regulation of rocks, deformation, and surface movement in multiseam strip mining process.

Filling mining is a mining technology that replaces coal pillar by filling body [11], which can effectively alleviate surface subsidence and deformation. Zhang et al. [12] constructed the in situ filling mining mode of coal gangue underground sorting based on underground sorting. Moreover, Guo et al. [13] proposed a new idea of three-step mining subsidence control: strip mining-grouting filling consolidation goaf-residual strip mining. Dai et al. [14] and Guo [14, 15] proposed a subsidence control mechanism of mining that is coordinately mixed with keeping and backfilling, and given the corresponding surface subsidence prediction formula. Based on the change of filling position and filling material elements, Xu et al. [16, 17] proposed the strip filling technology in goaf. The isolated grouting filling technology in separated strata and the grouting filling technology in caving zone of strip mining are suggested. Combined with the key strata theory, the control mechanism of strata in partial filling mining was revealed. The field practice shows that strip filling is an efficient and low-cost filling coal mining technology [18].

In summary, the strip mining resource recovery rate is low, while the filling mining cost is high. Therefore, the reliability of overburden strata control needs to be improved. The strip filling mining combines the benefits of filling mining and strip mining. Through reasonable design and layout of the coal pillars, filling working face, and caving working face, this not only ensures the resource recovery rate, but also achieves the goal of protecting human settlements and ecological environment. Moreover, appropriate monitoring systems will ensure safety in mines, avoid damages, and mine closure [19, 20]. The efficiency of the monitoring system in such environments is of utmost importance. Nevertheless, it has good technical advantages, but it is still widely used in single coal seam. However, most of the production mines in the lower and middle reaches of the Yellow River have the occurrence characteristics of multicoal seams, and there are many ground buildings. After the completion of the first coal seam mining, it is worth exploring how to reasonably arrange the lower coal seams mining to realize the effective control of strata and surface movement and reduce the disturbance to buildings. Therefore, this article take the geological and mining conditions of a mine in the middle and lower reaches of the Yellow River as the research background and investigate it through numerical simulations. Combined with the mechanical structure and movement law of strata in multicoal seam strip filling mining, the surface cooperative deformation mechanism of "large mining thickness under insufficient mining" with small coal pillar stagger distance and "small mining thickness under sufficient mining" with large coal pillar stagger distance is revealed.

Based on the characteristics of multiseam mining and the spatial stagger relationship of coal pillars between coal seams in strip filling mining, the surface movement law and cooperative deformation mechanism of strip filling mining under different coal pillar stagger distance are studied. This can also provide reference for safe and efficient green mining of multiseam in the lower and middle reaches of the Yellow River. In this article, an IoT and cloud computing based architecture is offered in order to support the development of a digital and sustainable mining platform. Moreover, mine monitoring methods, using Internet of Things (IoT) and machine learning, pursue to develop a suitable atmosphere to avoid damages and mine closure with supreme efficacy. Accurate monitoring methods reduce these damages and optimize mining. The key contributions of the research carried out in this article are as follows:

(i) We investigate the influence of coal pillar stagger distance on surface movement of multicoal seam strip filling mining

(ii) We propose a mechanism of surface cooperative deformation under different coal pillar stagger distance

(iii) A data aggregation method is suggested that runs on the edge device and send only important data to the cloud for storage

(iv) An IoT and cloud computing-based architecture is offered in order to support the development of a digital and sustainable mining platform

The rest of the article is systematized in the following manner. In Section 2, we discuss related materials and research methods that will familiarize the readers with the research field being investigated in this article. The UDEC numerical simulation and the essential toolkits are illustrated in Section 3. A machine learning framework based on the edge computing system is proposed in Section 4. Furthermore, a data aggregation method is suggested that process the collected data and saves the required data.

Section 5 demonstrates the obtained results. The major outcomes of our research are summarized in Section 6. To end with, Section 7 concludes the article and provides few guidelines for future research.

2. Materials and Methods

2.1. Overview of the Study Area. The mine in the study area belongs to a mine in Shandong Province. The terrain in the mine field is flat, coal retention rate under village reached 100%, and the relocation is difficult. The main coal seams are 5# coal, 8# coal, and 12-1# coal, and the coal thickness is 2.95 m, 3.94 m, and 2.95 m. The coal seam spacing is 49 m and 43 m. The interval strata are mainly fine sandstone and sandy mudstone. The coal seam dip angle is about 10°, the loose layer thickness is 80 m, and the mining depth is 491–723 m.

According to the calculation method of each working face size of single coal seam mining unit [15], combined with the geological and mining conditions and actual production benefits in the study area, the optimal widths of caving working face, filling working face, and reserved coal pillar of each mining unit of 5# coal in the first coal seam were determined as 80 m, 90 m, and 70 m, respectively. The first mining unit was completed between January 2018 and June 2020.

At the same time, the surface movement was observed, and the layout of the observation station is shown in Figure 1. The measured outcomes show that the largest subsidence of the surface movement surveillance station of the inclined main section is positioned on the side of the partial caving face above the mining unit. As shown in Figure 2, the largest subsidence value of the surface is 152 mm, and the subsidence ratio under the geological and mining conditions in this area is about 0.05, which has little effect on the surface movement, and there is no apparent destruction to the surface buildings during mining.

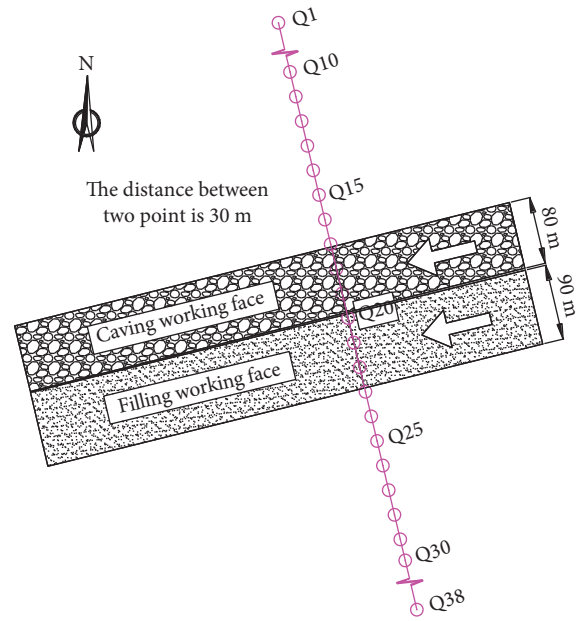

Figure 1: Observation station layout.

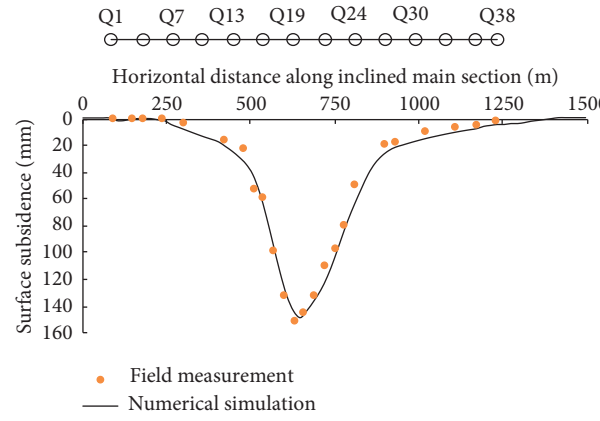

Figure 2: Comparison of field measurement and numerical simulation subsidence results in 5# coal mining (surface subsidence is measured in millimeter, and the distance is measured in meters).

2.2. Surface Cooperative Deformation Mechanism under Different Coal Pillar Stagger Distances. The staggered arrangement of coal pillar in multicoal seam strip filling mining includes multiple mining units of different coal seams, and each mining unit contains three components, namely caving face, filling face, and coal pillar. Coal pillar stagger arrangement according to the coal pillar stagger distance can be divided into coal pillar normal alignment, coal pillar part stagger, and coal pillar completely stagger, the specific arrangement is shown in Figure 3. The normal alignment arrangement of coal pillar is characterized by the alignment of coal pillar, filling working face, and caving working face of multilayer coal along the normal direction of coal seam [21]. In the layout mode of partial staggered coal pillar, the coal pillar, filling face, and caving face of multilayer coal are less than one coal pillar width transversely out of the upper coal; in the coal pillar completely staggered layout mode, the coal pillar, caving working face, and filling working face of multilayer coal are transversely deviated from a coal pillar width than the upper coal seam. In order to facilitate the study, based on the layout mode of coal pillar normal stagger change, the stagger degree is represented by coal pillar stagger coefficient s, and s is the ratio of coal pillar stagger distance l to coal pillar width a, the expression is $s = l/a \in [0, 1]$.

Overburden strata movement and surface subsidence are interrelated as a whole [22], and surface subsidence is the appearance of the movement and deformation of overlying strata in the surface. Strata movement includes arch, beam, and other structural forms [23, 24]. Different coal pillar stagger layouts have different mechanical bearing structures, and the surface movement characteristics will also be different.

The control of stagger layout mode on overlying strata and surface movement includes two dimensions, horizontal and vertical. In the horizontal direction, it shows that with the growth of stagger distance, the sufficiency of multicoal

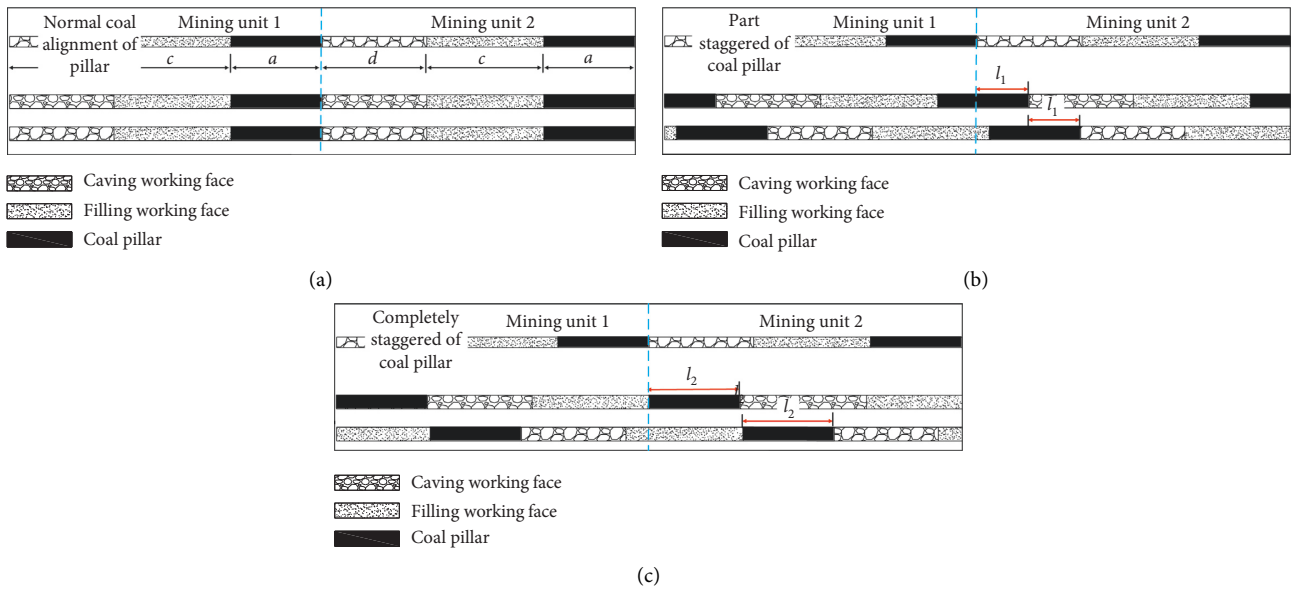

Figure 3: Diagram of the layout pattern of different coal pillar stagger distances.

seam mining increases. Vertically, the sequential layout of "coal pillar-filling working face-caving working face" avoids the large area suspension of roof. The smooth transition from coal pillar to caving working face can meritoriously diminish the separation space of the main key layer, and avoid the sudden chain failure instability of "domino effect" of the main key layer due to stress concentration. When the coal pillar is arranged in alignment or the stagger coefficient is small, the combination of coal pillar and filling body forms an effective bearing on the overlying strata, which blocks the connectivity of the caving areas on both sides. Multiple sets of stress arches are formed above the caving and filling working face, which are divided into multiple insufficient mining units.

At this time, the control effect on the surface is the best. With the increase of stagger distance, the effective combination of coal pillar and filling body support width decreases gradually, the sufficiency of mining increases, and the control effect of the surface is weakened. When reaching a certain critical value, the combination of coal pillar and filling body loses the main bearing function, and the mining units are connected to the rock failure zone, forming a flat arch across the three mining units above the mining area. At this time, the span and deflection of the main key layer are significantly increased, and the contact with the lower rock mass. The stress state of the overlying strata is changed from the local stress of the combination of coal pillar and filling body to the overall stress of the goaf [25]. The multiple mining units in the lateral space basically achieve sufficient mining, but are limited by the longitudinal comprehensive mining thickness. The separation space under the key layer is not enough to lead to structural breakage and can still play a role in controlling surface subsidence. The stagger distance continues to increase, similar to the sufficient mining stage of the working face, the surface subsidence changes little until it reaches the maximum.

The surface cooperative deformation mechanism of multilayer coal strip filling mining is shown in Figure 4. Affected by repeated mining of multiple coal seams, the strata and surface above the mining face experience multiple subsidence and the surface subsidence is the superposition of surface subsidence of each mining face in adjacent mining units of different coal seams. As shown in Figure 4(a), when the coal pillar is arranged in a normal alignment, the goaf of the narrow caving face on both sides is effectively blocked by the combination of coal pillar and filling body. After the multilayer coal mining, it is equivalent to a mining unit with the same thickness or slightly larger than the sum of the mining thickness of each coal seam in space, forming a "large mining thickness of insufficient mining." However, the layout mode of fully staggered coal pillars (Figure 4(b)) is adopted. In this layout mode, the combination of coal pillar and filling body between coal seams loses the bearing capacity [26].

The damage to rock strata after multilayer coal mining is equivalent to a mining unit with large mining width and small mining thickness in space [27]. In other words, each caving face connected horizontally staggered arrangement forms a working face with large mining width, and the overall formation of "sufficient mining with small mining thickness." Simultaneously, with the growth of the coal seam stagger coefficient, the subsidence gradient of the surface basin is gradually reduced. When the stagger coefficient is large, the tensile and compression deformation area is superimposed after mining between coal seams, and the surface deformation value of the central goaf is small, which is beneficial to the safe use of buildings. The partial stagger arrangement is in the transition stage of the above two cooperative deformation structures from overburden to surface.

3. UDEC Numerical Simulation

3.1. Principles of the UDEC. The UDEC is a two-dimensional discrete element numerical simulation software developed by ITASCA for the treatment of discontinuous media, all

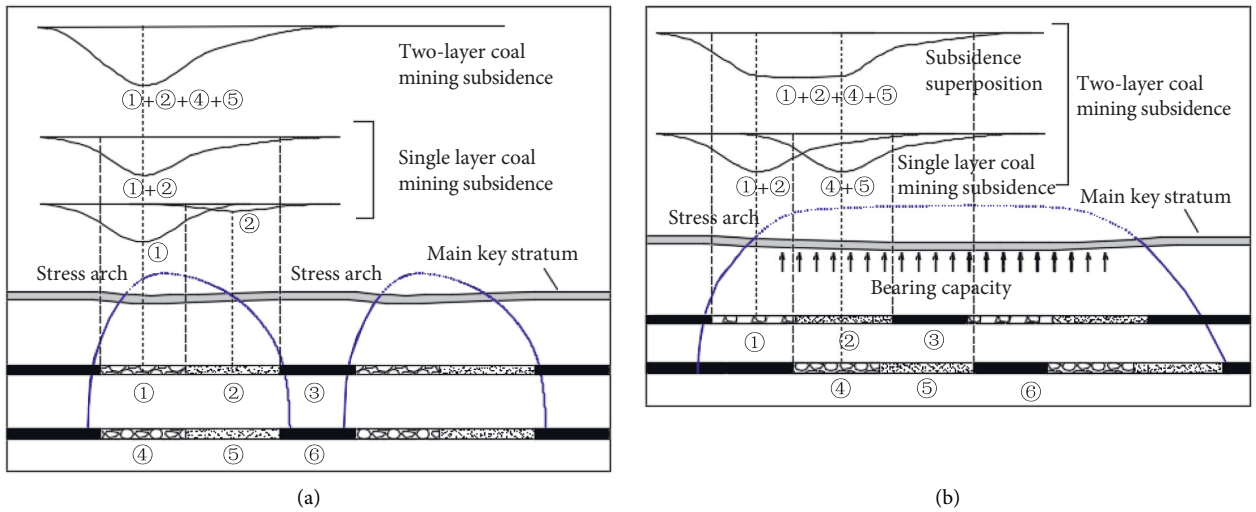

Figure 4: Surface cooperative deformation mechanism under different coal pillar stagger distances. (a) Normal alignment of coal pillars ($s = 0$). (b) Completely staggered coal pillars ($s = 1$).

known as Universal Distinct Element Code. In fact, the UDEC can be used to mimic and simulate the reaction of discontinuous media (for instance, joints in rock mass) under static or dynamic loads. The discrete block set is used to represent the discontinuous medium, and the boundary surface between blocks is used to represent the discontinuous surface, allowing large displacement and rotation of blocks along the discontinuous surface, which can be used to simulate the displacement phenomenon that may occur at the discontinuous geological interface. In the recent years, UDEC has developed one of the most effective tools to investigate the mining subsidence problem [28].

3.2. Establishment of the Model. The UDEC software was used in the numerical simulation, and the geological and mining conditions of a mine in Shandong Province were taken as the prototype. According to the distribution of rock strata exposed by the mine drilling, the appropriate simplified modeling was carried out. The model size is 1800 m × 800 m, and the actual development and distribution of the discrete element block reference rock are divided into 20,550 units.

In the proposed model, three mining units are arranged for each layer of coal. The caving face, filling face, and coal pillar width of the first coal mining unit are the actual mining size of 5# coal, 80 m, 90 m, and 70 m, respectively; the mining sequence between coal seams is first up and then down, and the working face is first filling working face and then coving working face in the same group of mining units. The geometric model for numerical simulation of coal pillar normal alignment layout is shown in Figure 5. In the next subsections, we briefly elaborate the establishment of the proposed model.

3.2.1. Determination of Key Mining Parameters of Filling Working Face. In deep filling mining face, the filling rate and compaction rate of filling materials have a direct impact on the bearing capacity of column filling combination [29, 30], and it is also the key to control the deformation of strata and surface movement. Referring to the actual situation of the existing working face filling mining in the mining area, the simulation filling rate is 80% and the compaction rate is 85%.

3.2.2. Constitutive Model and Boundary Conditions. According to the material difference and the characteristics of UDEC software, the Mohr-Coulomb model reflecting the shear failure characteristics of the material is selected for the loose layer and the coal and rock mass in the model, and the double-yield model reflecting the low-bond granular material is used for the filling body [15]. The surface contact Coulomb sliding model is selected for the joints. The upper boundary of the model is a free surface, and the left and right boundary conditions are applied to limit the horizontal displacement. The lower boundary is a fixed support, and the displacement in the horizontal and vertical directions is limited. The initial stress field is the self-weight stress of the stratum.

3.2.3. Determination of Numerical Simulation Parameters Based on the Mined Working Face. Based on the laboratory mechanical measurement, the mechanical as well as the physical characteristics and parameters of rock mass and coal are determined through comprehensive comparison with the measurement of field of the mining face. Combined with laboratory measurements and empirical parameters, the mechanical and physical factors and parameters of numerical simulation rock mass and coal are preliminarily determined. The obtained outcomes are illustrated briefly, as shown in Table 1; and the model of 5# coal seam mining unit 1 excavation is the most effective.

Figure 2 shows the comparison of the subsidence results of field measurement and numerical simulation after 5# coal mining.

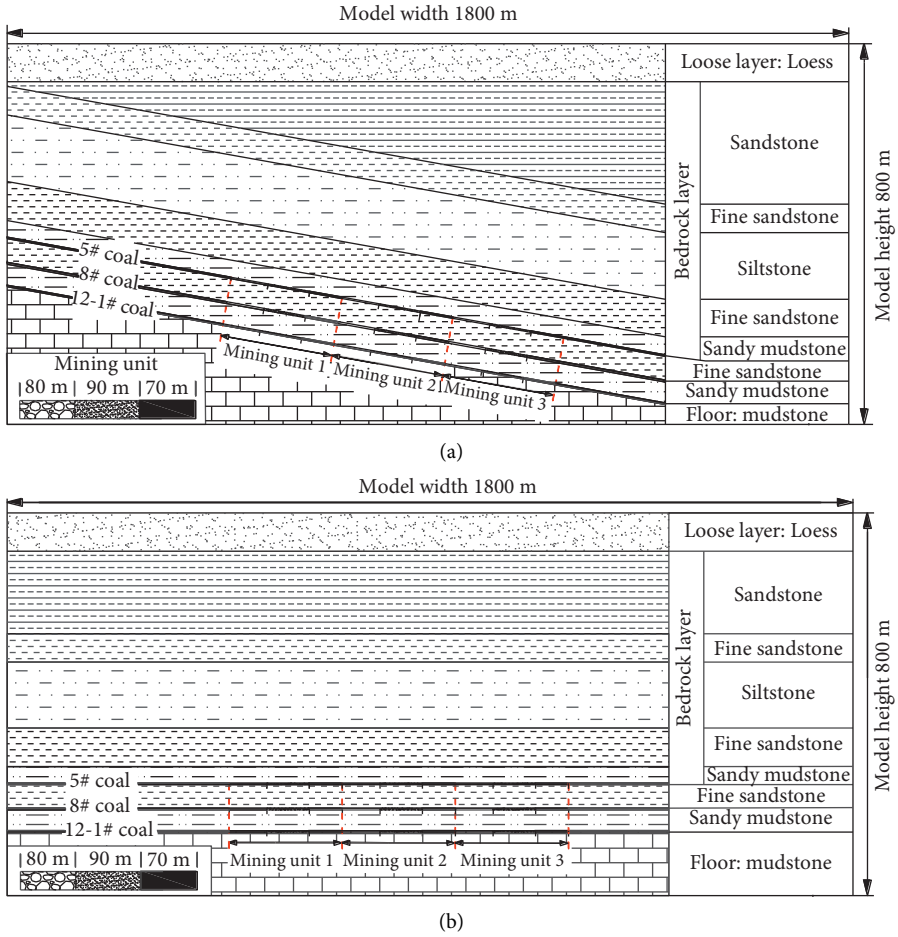

Figure 5: Geometric model for numerical simulation of the coal pillar normal alignment layout. (a) Arrangement along the inclination ($\alpha = 10^{\circ}$). (b) Arrangement along the strike of coal seam ($\alpha = 0^{\circ}$).

Table 1: The mechanical and physical parameters of the coal rock in the UDEC model.

Lithology	Thickness (m)	Density ($kg \cdot m^{-3}$)	Bulk modulus (GPa)	Shear modulus (GPa)	Cohesion (MPa)	Friction angle (°)	Tensile strength (MPa)
Loess	80	1800	0.67	0.3	0.20	20	0.12
Sandstone	183	2462	15.7	5.9	0.25	31	0.20
Fine sandstone	59	2662	35.2	7.4	0.38	34	0.21
Siltstone	138	2627	26.4	5.1	0.48	34	0.24
Fine sandstone	81	2662	35.2	7.4	0.38	37	0.21
Sandy mudstone	34	2500	9.14	2.1	0.57	35	0.45
5# coal	2.95	1400	0.90	0.8	0.28	25	0.10
Fine sandstone	49	2500	9.14	1.9	0.38	35	0.21
8# coal	3.94	1400	0.90	0.8	0.28	25	0.10
Sandy mudstone	34	2500	9.14	2.1	0.57	35	0.45
12-1# coal	2.95	1400	0.90	0.8	0.28	25	0.10
Mudstone	143	2700	45.1	7.8	0.60	30	0.24

It can be seen from Figure 2 that the simulated maximum subsidence value of the surface is 148 mm, which is close to the field measured maximum subsidence value. The mean error between the simulated subsidence and the field measured surface is 10.2 mm, and the relative error is 6.7%, which verifies the mechanical parameters of the numerical model and the reliability of the simulation calculation. Therefore, this set of parameters is adopted in the

subsequent excavation of other mining units of 5# coal and other simulation schemes.

3.3. Numerical Simulation Scheme. Multiple coal seam mining involves many geological mining factors, such as mining thickness, mining depth, coal seam spacing, and overburden lithology. For specific projects, the geological conditions are fixed. Therefore, in order to study the law of strata and surface movement of different coal pillar offset modes in multiseam strip filling mining, this section changes the normal stagger distance of coal pillars on the basis of the strip filling mining of single coal seam, and establishes the simulation schemes of different coal pillar stagger layouts ($s = 0$, 0.25, 0.5, 0.75, 1) when the multicoal seam mining is arranged along the strike ($\alpha = 0^{\circ}$) and along the incline ($\alpha = 10^{\circ}$).

4. Internet of Things (IoT) and Cloud-Based Monitoring and Prediction System

The prominence of the IoT, cloud computing, and communication technologies in sustainable mining platform cannot be exaggerated. In fact, this setup can deliver connectivity between various sensing, data collection units, and monitoring modules of the IoT prototype and, therefore, could allow real-time decision making through integration of various components. The most popular methods for avoiding mining dangers and equipment damage are monitoring and early warning. IoT-based monitoring devices now provide extensive data, thanks to the growth of the IoT and edge computing, improving the accuracy and efficiency of early warning and mining monitoring. Additionally, IoT monitoring data might be directed to a remote centralized cloud facility for computational processing in order to produce reliable data sources for timely warning. Nevertheless, the overwhelming volume of IoT devices uses up the majority of the cloud center's resources, lengthening the time it takes to analyze data. Furthermore, a constrained bandwidth prevents the transmission of a lot of monitoring data. As a result, cloud computing occasionally falls short of the real-time demands of prompt and timely warning. Monitoring data may be processed quickly with edge computing technology since it processes data more locally than at a centralized cloud center. The wide-ranging prototype of edge-based IoT data mining for prevention, particularly monitoring and timely warning, is shown in Figure 6 [31].

Usually, edge servers reside between the client and the cloud that play a major role when latency and speed of the decision making is important. For example, in the case of prediction, the training module will learn from the huge amount of data that is not possible at the client or edge. Similarly, when collecting the data, it might not be possible to store all the data on the client or edge. Therefore, the mining and geological data can be stored over the cloud and can be accessed through any communication medium. In fact, this architecture can be used as part of the monitoring

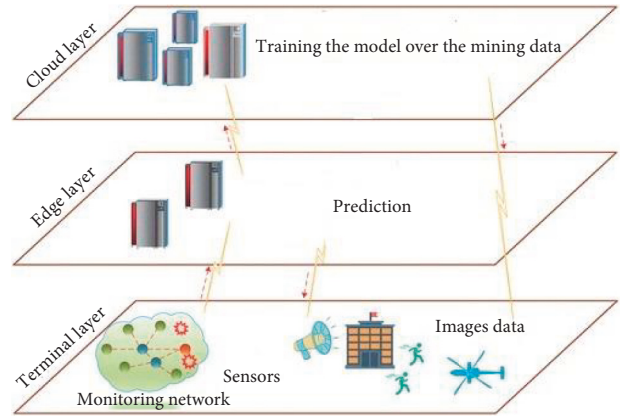

Figure 6: IoT edge mining monitoring and data processing system.

system in any physical mining cite for human and environmental safety.

The above IoT edge architecture is then used to implement the deep learning method as shown in Figure 7. Deep learning techniques are very time-consuming, in particular, when images data are taken into account. Literature suggests that deep learning method such as GCN (graph convolutional network) is largely used in scenarios when the data are mentioned in images, and that is the case in mining. Therefore, to reduce the prediction time, the training may happen at the cloud that are resource rich, while the prediction module can be executed in the edge that has limited resources. Note that, images data are collected through camera and sensors. To further improve and clean the data, data fusion and aggregation methods can be used to reduce the amount of data. Such prediction decisions can be either related to human safety or environmental disasters which may occur in the mining cites. Deep learning models are time-consuming and it may take quite long. Therefore, the proposed IoT edge platform can be used to expedite the decision making. This should be kept in mind that failure to deliberate the observing in active working face, goaf, and other areas in mining decisions consequences in mining accidents.

4.1. The Data Aggregation Method. The proposed edge model can further be enhanced through using an aggregation method. This is due to the fact that edge resources are small and cannot process huge data. Therefore, it would be essential to reduce the amount of data. However, the aggregation algorithm reduces the data points, therefore, less data means lower accuracy and vice versa. Initially we gather data and process it grounded on the proposed data aggregation system. In fact, numerous IoT devices that can quantify and monitor the physical mining environment and observe real-time environment deviations make up the terminal layer as shown in Figure 6. Data that have been gathered by multiple sensors that are positioned over similar areas may be redundant. Only meaningful data must be stored, which requires a procedure. The IoT ecosystem uses a large number of sensors to gather data, and the reporting

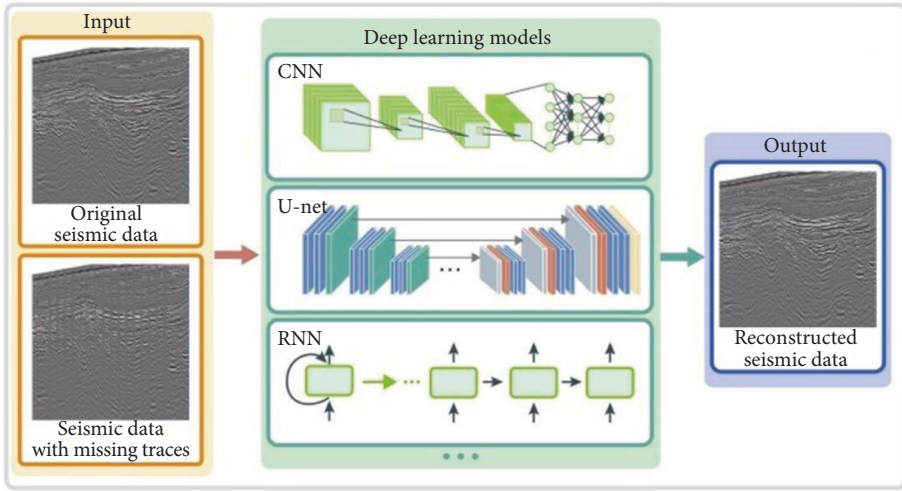

Figure 7: Deep learning model for training and prediction for mining monitoring [31].

area is expected to commonality. Due to this commonality, identical, pointless data may be gathered, which may place a strain on the server or other storage medium. Subsequently, this may also lead to strain the machine learning algorithm. Time spent training and hence predicting can be squandered in addition to latencies lengthening. Due to network congestion and prediction process impairment, the massive amount of data collected may contain duplicate values. Duplicate data must therefore be eliminated using a process. One of the i or j values is maintained while the other is eliminated if the ratio of $D_{\min}$ to $D_{\max}$, as illustrated by Equations (1) and (2), respectively, is less than the predetermined threshold value, indicating that the data are identical. Both data points must be included throughout the assessment process if the ratio of $D_{\min}$ and $D_{\max}$ is larger than or identical to certain predefined threshold value, indicating that the data are divergent.

$$D_{\min} = \sqrt{\left(\min_j - \min_i\right)^2} \text{ for all } i, j = 1 \ldots n, \tag{1}$$

$$D_{\max} = \sqrt{\left(\max_j - \max_i\right)^2} \text{ for all } i, j = 1 \ldots n. \tag{2}$$

The best time for aggregation is during the data collection phase. The technique and the pseudocode for aggregating data points are demonstrated in Algorithm 1. We calculate the Euclidean distance for each data point through step 1 to step 4. In steps 5–7, we compare the data point's value to a threshold value that has been predetermined. In case if the given conditions are satisfied, then the data point is eliminated; if not, then the algorithm continues on to the subsequent data point. Note that this is significant to remember that the datasets must be standardized before the Euclidean distance metric can be applied. A streamlined normalizing function must be used to ensure the application of the aforementioned distance metric. In this research, we used the normalizing technique outlined by

$$M_i^{\text{norm}} = \frac{M_i - M_{\min}}{M_{\max} - M_{\min}}, \tag{3}$$

where M_i^{norm} is a normalized value for M_i and $M_{\min}M_{\max}$ are the smallest and largest values through all data points, correspondingly. For instance, we might use $M_{\min} = 0$ and $M_{\max} = 1$ to normalize the supplied data points in a dataset within the range of 0 and 1. In this method, the threshold should be appropriately defined since it will affect the ratio of the discarded data. The above method is largely used due to its lower computational costs and we believe that the edge resources are quite enough to run this algorithm.

5. Results and Discussion

From Figures 8 and 9, it can be seen that when the coal pillar is arranged in normal alignment, that is, when $s = 0$, the subsidence of rock in each caving-filling working face propagates independently to the surface. The overlying strata subsidence above the coal pillar is slight, indicating that the coal pillar itself is stable due to the lateral protection of the filling body, which can support the roof and isolate the adjacent caving-filling working faces. At this time, the surface subsidence above the coal pillar is smaller than that of the caving-filling working face, and the central subsidence basin is wavy, with the maximum subsidence value of 2066 mm.

When the coal pillar stagger coefficient $s = 0.25, 0.5$, with the increase of coal pillar stagger coefficient, the superimposed area of coal pillar in upper and lower coal seam decreases, and the strata movement in the adjacent caving-filling working face is gradually connected to each other. The subsidence range of rock is getting larger and larger, and the subsidence value increases. The strata above the coal pillar is affected by the caving-filling working face on both sides, and the subsidence difference between the rock above the coal pillar and the caving-filling working face is reduced. The isolation effect of the coal pillar is weakened. In terms of

Input: Original dataset denoted by points P_i and P_j
Output: Refined dataset denoted by two points P_i' and P_j'
(1) for each element i, j in P_i, P_j
(2) if $j \leq i$ or $i \notin P_i$ or $j \notin P_j$
(3) Do nothing [no duplicate data]
(4) end if
(5) $E_d(P_i, P_j) = \sqrt{(p_{ik} - \min_{jk})^2}$ where $p_{ik} \in P_i$ and $p_{jk} \in P_j$
(6) if $E_d(P_i, P_j) \leq T_d$ then
(7) Discard either P_i or P_j, to form P_i' or P_j'
(8) end if
(9) return P_i' or P_j'

Algorithm 1: The data aggregation algorithm based on the Euclidian distance.

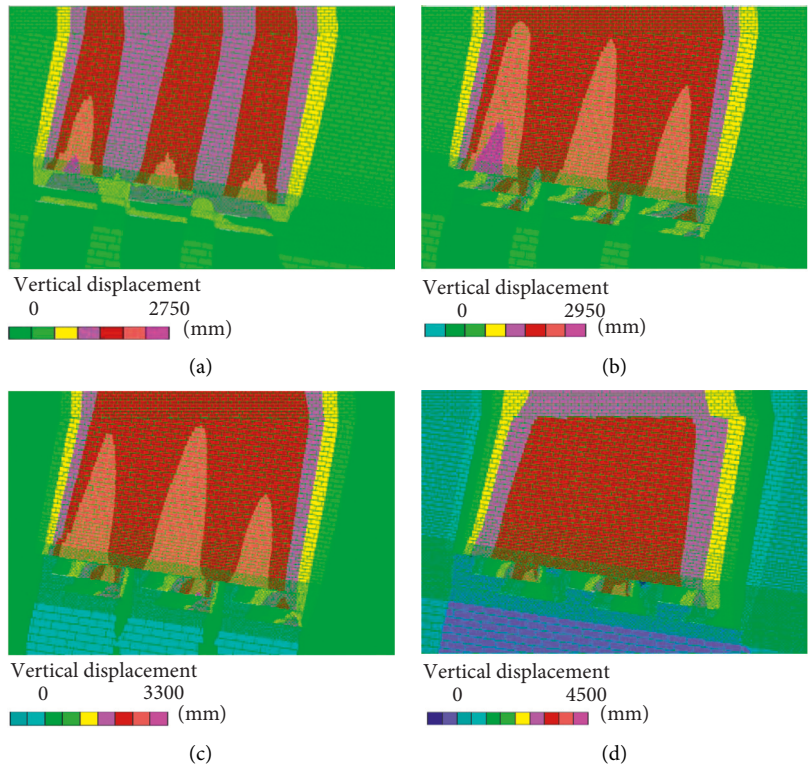

Figure 8: The vertical displacement nephogram of strata on numerical simulation scheme (for $\alpha = 10^\circ$ and $s = 0$, 0.25, 0.5, 1). (a) $s = 0$. (b) $s = 0.25$. (c) $s = 0.5$. (d) $s = 1$.

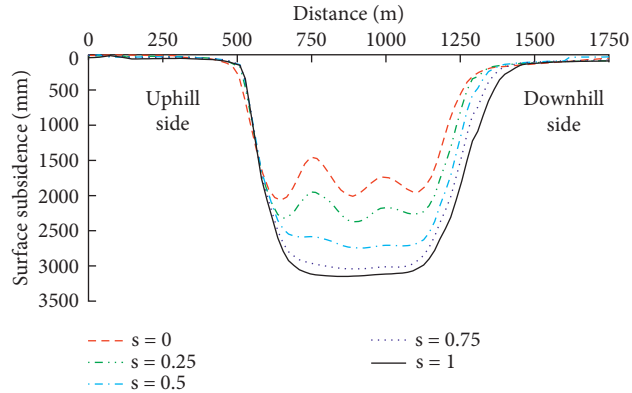

Figure 9: Surface subsidence curve of mining with staggered layout mode (surface subsidence is measured in millimeter, and the distance is measured in meters).

surface subsidence, with the increase of the coal pillar stagger coefficient, the surface subsidence values of the caving-filling working face and above the coal pillar increase. At the same time, the subsidence gradient at different positions in the center of the basin decreases, and it begins to transform from wavy subsidence to uniform subsidence.

When the coal pillar stagger coefficient $s = 0.75$, 1, the coal pillar stagger coefficient continues to increase, the adjacent strata movement area overlaps on the mining face, the "pointed tower" subsidence area on the mining face with small coal pillar stagger disappears, and the subsidence of each rock layer above the central mining area tends to be consistent, and the subsidence range and subsidence value of the rock continue to increase. The center of the surface subsidence basin completely becomes uniform subsidence. When the coal pillar stagger coefficient $s = 1$, the surface subsidence reaches the maximum of 3149 mm.

5.1. Impact of the Number of Coal Seams Mined on Surface Movement. The surface movement law changes with the increase of coal seam number under different coal pillar normal offset layout mode. The maximum surface subsidence and the maximum horizontal movement of the three-layer coal after mining in turn under different coal pillar normal stagger layout modes are shown in Figure 10.

From Figure 8, it can be seen that the maximum subsidence value and maximum horizontal movement value of the surface increase with the increase of mining layers. When the coal pillar is normal aligned, the maximum surface subsidence value is 575 mm and the maximum horizontal movement is 154 mm after the first coal seam 5# coal mining. With the mining of 8# coal and 12-1# coal, the cumulative mining thickness of coal seam increases, and the maximum surface subsidence and maximum horizontal movement increase. At this time, the maximum surface subsidence value of coal pillar normal alignment ($s = 0$) is 2066 mm, and the maximum horizontal movement is 187 mm. When the coal pillar is completely staggered ($s = 1$), then the supreme surface subsidence is approximately 3149 mm, the supreme horizontal movement is 255 mm, and the maximum surface subsidence rises by 1491 mm and 2574 mm, respectively.

Combined with the analysis in Figures 6 and 8, it can be comprehended that under different coal pillar normal offset modes, the increase in the number of coal seams has different effects on surface movement. After the first floor 5# coal mining is completed, with the mining of 8# coal and 12-1# coal, there are many disturbances on the surface and the movement deformation value increases. When the offset coefficient $s < 0.75$, the mining area is relatively concentrated in the longitudinal direction, showing the characteristics of insufficient mining, and multiple small basins are formed on the surface. When the coal pillars are aligned in the normal direction, the surface subsidence rate of multicoal seam mining is only 0.210. When the stagger coefficient $s \geq 0.75$, the multilayer coal mining face overlaps in the longitudinal direction

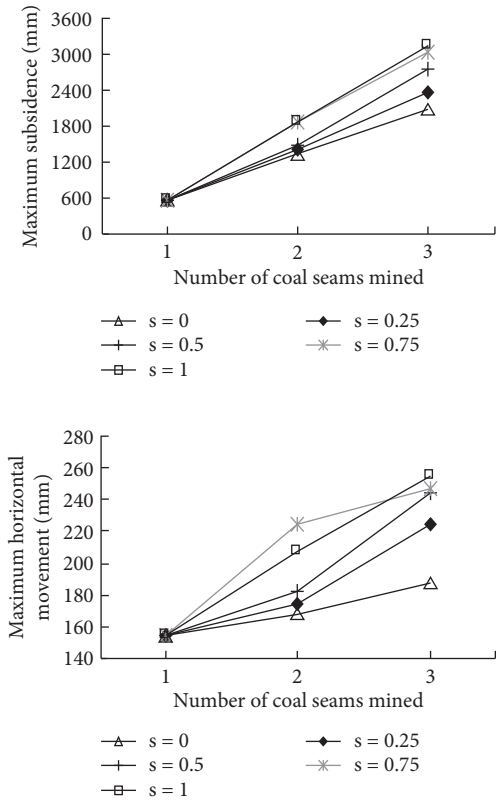

Figure 10: Relationship between the maximum surface movement and the number of mining layers under layout patterns of different staggered coal pillars (horizontal coordinates 1 for mining 5# coal single layer; 2 for mining 5# coal and 8# coal two layers; 3 for mining 5# coal, 8# coal, and 12-1# coal three layers).

and the subsidence area is gradually connected. The adequacy of horizontal mining increases, and the maximum subsidence value of the surface is large, showing the characteristics of "full mining." The surface subsidence curve is connected from multiple small basins to the overall subsidence basin. The surface subsidence ratio of each staggered layout mode of multicoal seam strip filling is 0.21–0.32, which is smaller than that of multicoal seam caving mining ($q_c = 0.6$) [32], effectively alleviating the surface subsidence and beneficial to the protection of surface buildings.

5.2. Influence of Coal Pillar Stagger on Surface Movement. With the increase of coal pillar offset coefficient, the changes of surface subsidence rate and horizontal movement coefficient after three-layer coal mining are shown in Table 2.

When the normal alignment of coal pillars $s = 0$, the surface subsidence ratio is the smallest. After the three-layer coal mining, the surface subsidence rate is 0.210. When the coal pillars are completely staggered, namely $s = 1$, the surface subsidence rate is the largest, and the subsidence rate is 0.320, which is 1.5 times that of the normal alignment of coal pillars.

Combined with Table 2 and Figure 11, it can be seen that the maximum surface subsidence value and subsidence rate

Table 2: Surface movement value of strip filling mining in multiseam with different coal pillar normal direction staggers ($\alpha = 10^{\circ}$, $q = W_{max}/M\cos\alpha$, $b = U_{max}/W_{max}$).

Coal pillar stagger coefficient	Maximum subsidence W_{max} (mm)	Subsidence ratio q	Maximum horizontal movement U_{max} (mm)	Horizontal movement coefficient b
$s = 0$	2066	0.210	187	0.09
$s = 0.25$	2371	0.241	238	0.10
$s = 0.50$	2745	0.279	245	0.09
$s = 0.75$	3041	0.309	247	0.08
$s = 1$	3149	0.320	255	0.08

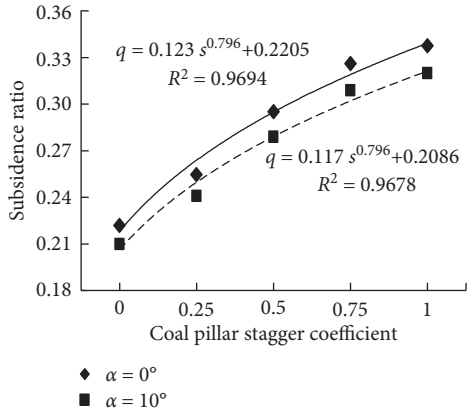

Figure 11: Relationship between subsidence ratio and coal pillar stagger coefficient (fitted with power function having 96.78% and 96.94% accuracies).

are positively correlated with the coal pillar offset coefficient. The relationship between surface subsidence rate and coal pillar offset coefficient is approximately a power function. The surface horizontal movement coefficient increases first and then decrease with the increase of coal pillar offset coefficient, and gradually tends to be stable, about 0.09. Under the geological and mining conditions of the mine, when the offset coefficient reaches a certain value ($s \geq 0.75$), the surface subsidence and horizontal movement are less affected by the change of coal pillar offset. Through regression analysis, the empirical relationship between surface subsidence ratio and coal pillar offset coefficient in multiseam strip filling mining is established: $q = 0.117s^{0.796} + 0.2086$, the goodness of fit $R^2 = 0.968$.

5.3. Difference of Surface Subsidence along Strike and Inclination of the Working Face. The numerical simulation outcomes illustrate that the whole influence range of multicoal seam strip filling mining surface is minor or tiny, and the subsidence is mainly concentrated in the mining area along the normal direction. Among them, the subsidence basin after the mining of the working face is symmetrically distributed along the strike. When the working face is arranged along the incline direction, then the steep degree of the uphill direction is slightly larger than that of the downhill direction. However, the settlement range is smaller than that of the downhill direction, as presented in Figure 9.

Figure 11 presents the surface subsidence ratio of mining with various stagger coefficient of coal pillars along the strike and inclination of the working face. We can clearly observe from the figure that the surface movement law of the working face along the strike ($\alpha = 0^{\circ}$) and along the inclination ($\alpha = 10^{\circ}$) is the same under different coal pillar normal stagger modes, and the subsidence ratio and coal pillar stagger coefficient are in a power function relationship. On the settlement value, the surface subsidence along the strike arrangement is larger than that along the inclination, and the surface subsidence rate increases by about 7%. It indicates that under the condition of gently inclined coal seam, the layout of working face along the incline direction will slow down the surface subsidence to a certain extent. This is consistent with the idea that the mining area chooses the mining plan along the inclination.

5.4. Results of the Machine Learning and Aggregation Methods. We implemented three different machine learning algorithms, that is, CNN, RNN, and U-net [33], where the training happens on a cloud and prediction at the edge. The U-net method is implemented along with the attention mechanism. The outcomes of different approaches and their accuracies with and without the aggregation method are given away in Figures 12 and 13, one-to-one. As shown in Figure 12, for various algorithms, the aggregation method considerably diminishes the model execution times. For training period, we observed approximately 38.8% to 40.9% improvement. Similarly, for prediction period, the improvement was observed up to 14.2% to 18.9%. Note that the time is represented in seconds. Nevertheless, neither CNN nor U-net could reduce the prediction times significantly and they produced almost comparable outcomes. As shown in Figure 13, the aggregation methodology formed worst outcomes in terms of prediction precision and correctness, that is, MAPE and RMSE metric values. However, the RNN approach produced comparable results. This shows that, for RNN, our proposed method has significantly learned well even from the small-scale dataset. This also demonstrates that when the data are less, the accuracy of the learning approach will be small and vice versa. The MAPE values are mentioned in percentage (%), while the RMSE factor denotes a number. The minor values exemplify a higher precise system, while the bigger values denote less accuracy.

6. Major Findings

The following are the major findings of our research:

(i) The surface cooperative deformation mechanism of different coal pillar stagger distance in multicoal

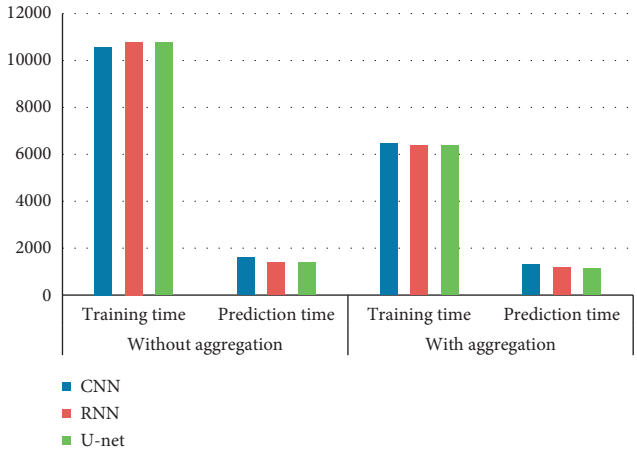

Figure 12: Comparison of training and prediction times for three different algorithms with and without the aggregation technique.

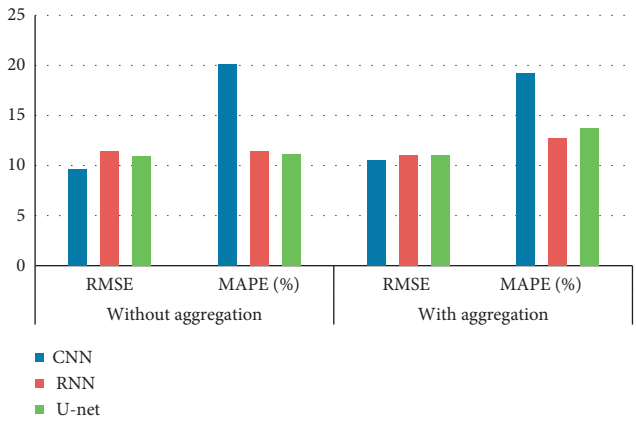

Figure 13: Accuracy of the three machine learning methods in terms of RMSE and MAPE with and without the aggregation technique.

seam strip filling mining is revealed. Through the coordination of the spatial positions of multiple mining units, the effective bearing structure of the combination of coal pillar and filling body is formed. Furthermore, the mining space of the upper and lower coal seams is controlled, so as to reduce the movement space of the main key strata and control the surface subsidence. Acting on the surface, the movement and deformation characteristics of "large mining thickness under insufficient mining" with small coal pillar stagger distance and "small mining thickness under sufficient mining" with large coal pillar stagger distance are formed.

(ii) Using the method of numerical simulation, the influence of different coal pillar stagger distance in multiseam mining on surface movement is studied. Surface subsidence is positively correlated with coal pillar stagger coefficient and mining layers. With the increase of the normal stagger of coal pillar, the support width of the effective combination of coal pillar and filling body decreases, and the sufficiency of horizontal mining increases. The overlying strata subsidence on each caving-filling working face gradually tends to be uniformly transmitted from independent propagation. The central surface subsidence basin changes from wavy subsidence to uniform subsidence, and the subsidence gradient and deformation value decrease.

(iii) The surface subsidence ratio of multicoal seam strip filling mining is power function with the coal pillar stagger coefficient, the subsidence ratio is about 0.21–0.32 and the horizontal movement coefficient is about 0.09. When the coal pillar is aligned, namely $s = 0$, the maximum surface subsidence is 2066 mm and the control effect is the best. When the stagger coefficient $s \geq 0.75$, the surface subsidence and horizontal movement are less affected by the change of coal pillar stagger. Regression analysis established the fitting formula of surface subsidence ratio and coal pillar stagger coefficient.

(iv) The mining conditions of gently inclined coal seam and the arrangement of working face along the incline direction can slow down the surface subsidence to a certain extent, which is beneficial to the protection of surface buildings.

7. Conclusions and Future Work

Mine monitoring methods, using Internet of Things (IoT), pursue to develop a suitable atmosphere to avoid damages and mine closure with supreme efficacy. Accurate monitoring methods reduce these damages and optimize mining. Strip filling mining is characterized by high efficiency, reliability, and low cost, which provides a good technical support for mining damage control. However, how to reasonably layout the working face under multicoal seam conditions and the law of surface movement under different coal pillar stagger distance need to be studied. Based on the geological and mining conditions of a mine in Shandong Province, through numerical simulation and theoretical analysis, this article studies the influence of coal pillar stagger distance on surface movement of multicoal seam strip filling mining and reveals the mechanism of surface cooperative deformation under different coal pillar stagger distance. Furthermore, an IoT and cloud computing based architecture is offered in order to support the development of a digital and sustainable mining platform. The results show that the surface subsidence is positively correlated with coal pillar stagger coefficient and mining layers.

In the future, we will consider deep leaning approaches, such as graph convolutional network (GCN), that are more suitable for the mines and the monitoring systems that are operating there. Nevertheless, we witnessed that the activation function which was used in this article cannot stimulate all neurons that leads to limited precision and accuracy. Consequently, the search for the optimal activation function and the optimization of the model structure are further research work. Similarly, we will investigate the impacts of the activation functions which is used along with

the deep learning methods. Moreover, robust data reduction or aggregation methods should be investigated to improve the performance of the proposed system.

Data Availability

The raw/processed data required to reproduce these findings cannot be shared at this time as the data also form part of an ongoing study.

Conflicts of Interest

The authors declare that they have no conflicts of interest.

Acknowledgments

This research was financially supported by the Shanxi Graduate Education Innovation Project of China under grant number 2019SY126.

References

[1] S. P. Peng and Y. L. Bi, "Strategic consideration and core technology about environmental ecological restoration in coal mine areas in the Yellow River basin of China," *Journal of China Coal Society*, vol. 45, no. 4, pp. 1211–1221, 2020.

[2] Q. S. Li, Z. W. Zhang, and P. Z. Nan, "Mining impact pattern of mutil-coal seam," *Journal of China Coal Society*, vol. 31, no. 4, pp. 425–428, 2006.

[3] W. B. Guo, Z. B. Ma, and E. H. Bai, "Current status and prospect of coal mining technology under buildings, water bodies and railways, and above confined water in China," *Coal Science and Technology*, vol. 48, no. 9, pp. 16–26, 2020.

[4] Y. F. Zou, *Three-dimensional Layered Medium Theory of Strip Mining Optimization Design and Surface Subsidence Prediction*, Science Press, Beijing, 2011.

[5] X. C. Wang, F. C. Huang, H. X. Zhang, and L. G. Zhang, "Discussion and improvement for A.H.Wilson's coal pillar design," *Journal of China Coal Society*, vol. 27, no. 6, pp. 604–608, 2002.

[6] W. B. Guo, "Surface movement predicting problems of deep strip pillar mining," *Journal of China Coal Society*, vol. 33, no. 4, pp. 368–372, 2008.

[7] Y. Yu, S. E. Chen, K. Z. Deng, and H. D. Fan, "Long-term stability evaluation and pillar design criterion for room-and-pillar mines," *Energies*, vol. 10, no. 10, p. 1644, 2017.

[8] Y. Yu, K. Z. Deng, and S. E. Chen, "Mine size effects on coal pillar stress and their application for partial extraction," *Sustainability*, vol. 10, no. 3, p. 792, 2018.

[9] K. Z. Deng, W. M. Ma, and G. Q. He, "Influence of stripe space position on strata movement in multiple coal seams mining," *Journal of China University of Mining & Technology*, vol. 20, no. 2, pp. 75–81, 1991.

[10] J. Y. Zhang, "Theoretic study by simulation method on the strip mining of multiple coal seams," *Journal of China Coal Society*, vol. 25, no. S1, pp. 67–70, 2000.

[11] X. K. Sun and X. H. Li, "The new technology of waste-filling replacement mining on strip coal pillar," *Journal of China Coal Society*, vol. 33, no. 3, pp. 259–263, 2008.

[12] J. X. Zhang, F. Ju, M. Li, N. Zhou, and Q. Zhang, "Method of coal gangue separation and coordinated in-situ backfill mining," *Journal of China Coal Society*, vol. 45, no. 1, pp. 131–140, 2020.

[13] G. L. Guo, Y. H. Wang, and Z. G. Ma, "A new method for ground subsidence control in coal mining," *Journal of China University of Mining & Technology*, vol. 33, no. 2, pp. 150–153, 2004.

[14] H. Y. Dai, J. T. Guo, Y. G. Yan, P. X. Li, and Y. S. Liu, "Principle and application of subsidence control technology of mining coordinately mixed with backfilling and keeping," *Journal of China Coal Society*, vol. 39, no. 8, pp. 1602–1610, 2014.

[15] J. T. Guo, *Theory of Mining under Buildings with Mining Coordinately Mixed with Backfill Mining and Setting Pillars*, China University of mining and Technology, Beijing, 2014.

[16] J. L. Xu, W. B. Zhu, X. S. Li, and W. Q. Lai, "Study of the technology of partial-filling to control coal mining subsidence," *Journal of Mining & Safety Engineering*, vol. 23, no. 1, pp. 6–11, 2006.

[17] J. L. Xu, D. Y. Xuan, W. B. Zhu, X. Z. Wang, B. L. Wang, and H. Teng, "Study and application of coal mining with partial backfilling," *Journal of China Coal Society*, vol. 40, no. 6, pp. 1303–1312, 2015.

[18] Q. Chang, X. Yao, Q. Leng et al., "Strata movement of the Thick loose layer under strip-filling mining method: a case study," *Applied Sciences*, vol. 11, no. 24, p. 11717, 2021.

[19] X. G. Lian, Z. J. Li, H. Y. Yuan, H. F. Hu, Y. F. Cai, and X. Y. Liu, "Determination of the stability of high-steep Slopes by Global Navigation Satellite system (GNSS) real-time monitoring in long Wall mining," *Applied Sciences*, vol. 10, no. 6, p. 1952, 2020.

[20] K. Zhang, Q. S. Li, H. Y. Dai, J. T. Guo, and Y. G. Yan, "Research on integrated monitoring technology and practice of "space-sky-ground" on surface movement in mining area," *Coal Science and Technology*, vol. 48, no. 2, pp. 207–213, 2020.

[21] H. Yan, J. X. Zhang, S. Zhang, and N. Zhou, "Physical modeling of the controlled shaft deformation law during the solid backfill mining of ultra-close coal seams," *Bulletin of Engineering Geology and the Environment*, vol. 78, no. 5, pp. 3741–3754, 2019.

[22] Y. Zhang, F. He, J. Kong, Y. Zhu, and L. Wang, "Relationship between surface subsidence range and geological mining conditions using Numerical simulation and machine learning," *Scientific Programming*, vol. 2022, Article ID 8720831, 2022.

[23] Y. Zhang, Y. Yan, H. Dai, Y. Zhu, and T. Wu, "Stability and Force chain characteristics of "inclined StepCutting body" in Stope," *Applied Sciences*, vol. 11, no. 21, Article ID 10276, 2021.

[24] J. L. Xu and M. G. Qian, "Study on the influence of key strata movement on subsidence," *Journal of China Coal Society*, vol. 25, no. 2, pp. 122–126, 2000.

[25] H. Ebata, A. Yamamoto, Y. Tsuji et al., "Persistent random deformation model of cells crawling on a gel surface," *Scientific Reports*, vol. 8, no. 1, p. 5153, 2018.

[26] X. L. Yang, G. C. Wen, L. C. Dai, H. T. Sun, and X. L. Li, "Ground subsidence and surface cracks evolution from shallow-buried close-distance multi-seam mining: a case study in Bulianta coal mine," *Rock Mechanics and Rock Engineering*, vol. 52, no. 8, pp. 2835–2852, 2019.

[27] Z. J. Zhu, H. W. Zhang, J. Nemcik, T. W. Lan, J. Han, and Y. Chen, "Overburden movement characteristics of top-coal caving mining in multi-seam areas," *The Quarterly Journal of Engineering Geology and Hydrogeology*, vol. 51, no. 2, pp. 276–286, 2018.

[28] L. Wang, "Research on UDEC Numerical simulation of Upward mining in 42 Panel area of Wenjiapo mine," *Coal Technology*, vol. 40, no. 9, pp. 23–25, 2021.

[29] F. T. Wang, G. Li, J. G. Ban, X. N. Peng, S. T. Li, and S. F. Liu, "Synergistic bearing effect of backfilling body and coal pillar in deep mining," *Journal of Mining & Safety Engineering*, vol. 37, no. 2, pp. 311–318, 2020.

[30] Y. L. Huang, J. X. Zhang, Q. Zhag, S. J. Nie, and B. F. An, "Strata movement control due to Bulk factor of backfilling body in fully Mechanized backfilling mining face," *Journal of Mining & Safety Engineering*, vol. 29, no. 2, pp. 162–167, 2012.

[31] J. Qin, G. Mei, Z. Ma, and F. Piccialli, "General paradigm of edge-based internet of things data mining for geohazard prevention," *Big Data*, vol. 9, no. 5, pp. 373–389, 2021.

[32] G. Q. He, L. Yang, G. D. Ling, F. C. Jia, and D. Hong, *Mining Subsidence Theory*, China University of Mining and Technology Press, 1991.

[33] Y. Wang, J. Y. Kong, and H. S. Zhang, "U-net: a smart application with multidimensional attention network for remote sensing images," *Scientific Programming*, vol. 2022, pp. 1–11, 2022.